Smad4 deficiency impairs chondrocyte hypertrophy via the Runx2 transcription factor in mouse skeletal development

Received for publication, January 9, 2018, and in revised form, April 20, 2018 Published, Papers in Press, May 7, 2018, DOI 10.1074/jbc.RA118.001825

Jianyun Yan[‡§1], Jun Li[‡], Jun Hu[‡], Lu Zhang[‡], Chengguo Wei[¶], Nishat Sultana[‡], Xiaoqiang Cai[‡], Weijia Zhang[¶], and Chen-Leng Cai[‡2]

From the [‡]Department of Developmental and Regenerative Biology, The Mindich Child Health and Development Institute, and The Black Family Stem Cell Institute, Icahn School of Medicine at Mount Sinai, New York, New York 10029, the [§]Laboratory of Heart Center and Department of Cardiology, Heart Center, Zhujiang Hospital, Southern Medical University, Guangdong Provincial Biomedical Engineering Technology Research Center for Cardiovascular Disease, Sino-Japanese Cooperation Platform for Translational Research in Heart Failure, Guangzhou 510280, China, and the [¶]Renal Division of the Department of Medicine, Icahn School of Medicine at Mount Sinai, New York, New York 10029

Edited by Xiao-Fan Wang

Chondrocyte hypertrophy is the terminal step in chondrocyte differentiation and is crucial for endochondral bone formation. How signaling pathways regulate chondrocyte hypertrophic differentiation remains incompletely understood. In this study, using a *Tbx18:Cre* (*Tbx18*$^{Cre/+}$) gene-deletion approach, we selectively deleted the gene for the signaling protein SMAD family member 4 (*Smad4*$^{f/f}$) in the limbs of mice. We found that the *Smad4*-deficient mice develop a prominent shortened limb, with decreased expression of chondrocyte differentiation markers, including *Col2a1* and *Acan*, in the humerus at mid-to-late gestation. The most striking defects in these mice were the absence of stylopod elements and failure of chondrocyte hypertrophy in the humerus. Moreover, expression levels of the chondrocyte hypertrophy–related markers *Col10a1* and *Panx3* were significantly decreased. Of note, we also observed that the expression of runt-related transcription factor 2 (*Runx2*), a critical mediator of chondrocyte hypertrophy, was also down-regulated in *Smad4*-deficient limbs. To determine how the skeletal defects arose in the mouse mutants, we performed RNA-Seq with ChIP-Seq analyses and found that Smad4 directly binds to regulatory elements in the *Runx2* promoter. Our results suggest a new mechanism whereby Smad4 controls chondrocyte hypertrophy by up-regulating *Runx2* expression during skeletal development. The regulatory mechanism involving Smad4-mediated *Runx2* activation uncovered here provides critical insights into bone development and pathogenesis of chondrodysplasia.

Human chondrodysplasia is a heritable disorder affecting skeletal development, characterized by skeletal abnormalities with reduced length of the long bone and short stature. Several genetic mutations causing chondrodysplasia have been identified including type X collagen (*Col10a1*), runt-related transcription factor 2 (*Runx2*),[3] and cartilage-derived morphogenetic protein 1 (*CDMP1*) (1–4). These genetic mutations affect chondrogenesis crucial for endochondral bone development. Understanding the molecular pathways underlying chondrogenesis during skeletal development may provide crucial insights into the therapeutic treatments for chondrodysplasia in humans.

Endochondral ossification is an imperative developmental process for skeletal formation in vertebrates. Endochondral bone development is initiated by aggregation and condensation of mesenchymal cells. The mesenchymal cells further differentiate into primary chondrocytes with secreting type II collagen (Col2a1) and aggrecan (Acan) to form cartilage elements. Primary chondrocytes then proliferate and develop into hypertrophic chondrocytes that secrete Col10a1. Subsequently, hypertrophic chondrocytes are invaded by blood vessels and are replaced by bone and bone marrow (5–8). In this process, chondrocyte hypertrophy is a terminal step of chondrocyte differentiation, and is essential for endochondral bone formation. A few essential molecules that control chondrocyte hypertrophic differentiation have been found (9). Indian hedgehog (*Ihh*), a member of the hedgehog family, is expressed in prehypertrophic chondrocytes. Ihh is required for chondrocyte proliferation and chondrocyte hypertrophy (10, 11). Bone morphogenetic protein (BMP) family members are expressed throughout limb development and play vital roles in regulating chondrogenesis (12, 13). Deletion of *Bmp2* results in defective chondrocyte hypertrophy and endochondral bone formation, indicating Bmp2 is required for chondrocyte hypertrophic differentiation and endochondral bone formation (14). In addi-

This work was supported by National Institutes of Health Grants 1R01HL131735, 1R01HL095810, 1R56HL129807, and 1K02HL094688, American Heart Association Grants 15GRNT25710153 and 0855808D, and March of Dimes Foundation Grant 5-FY07-642 (to C. L. C.). The authors declare that they have no conflicts of interest with the contents of this article. The content is solely the responsibility of the authors and does not necessarily represent the official views of the National Institutes of Health.

This article contains Figs. S1 and S2 and Tables S1–S25.

The ChIP-Seq and RNA-Seq data can be accessed through the NCBI Gene Expression Omnibus (GEO) Repository using accession numbers GSE114081 and GSE114079, respectively.

[1] Supported by National Natural Science Foundation of China Grants 81470488, 81770280, and 81728004.

[2] To whom correspondence should be addressed: Dept. of Developmental and Regenerative Biology, The Mindich Child Health and Development Institute, and The Black Family Stem Cell Institute, Icahn School of Medicine at Mount Sinai, One Gustave L. Levy Place, New York, NY 10029. Tel.: 212-824-8917; E-mail: chenleng.cai@mssm.edu.

[3] The abbreviations used are: Runx2, runt-related transcription factor 2; CDMP1, cartilage-derived morphogenetic protein 1; Ihh, Indian hedgehog; BMP, bone morphogenetic protein; R-Smads, receptor-activated Smads; qRT, quantitative RT; GO, gene ontology; TSS, transcription start site; X-Gal, 5-bromo-4-chloro-3-indolyl β-D-galactoside; PFA, paraformaldehyde; EdU, 5-ethynyl-2′-deoxyuridine; ChIP-seq, ChIP-sequencing.

tion, Runx transcription factors Runx2 and Runx3 also regulate and coordinate chondrocyte hypertrophic differentiation and proliferation (15, 16).

Smad4 is a central mediator of canonical transforming growth factor (TGF)/BMP signaling (17) and it binds to receptor-activated Smads (R-Smads) and forms a complex with R-Smads. The Smad complex translocates into the nucleus and serves as a transcription factor to regulate the expression of targeting genes involved in a wide variety of development and homeostasis processes. During mouse embryogenesis, Smad4 is expressed in the developing limbs and is required for early mesenchymal cell aggregation, chondrocyte differentiation, osteoblast differentiation, and maturation (18–21). The regulatory mechanism of the Smad4 underlying chondrocyte hypetrophic differentiation during long bone development is unknown, although studies on TGF/BMP pathway genes showed that Bmp2 regulates *Runx2* expression through Smad in the C2C12 cell line (22), and Runx2 physically interacts with Smads in COS7 cells *in vitro* (23). In this study, we performed a genetic study in mice and found that loss of *Smad4* within the limb resulted in the absence of chondrocyte hypertrophy and ossification in humerus of mice. In addition, Smad4 promotes expression of hypertrophy differentiation genes, including *Runx2*, *Runx3*, and *Ihh*. Further RNA-seq and ChIP-seq analyses revealed that Smad4 regulates a wide spectrum of genes associated with limb development, including direct activation of *Runx2*. These findings reveal an important mechanism by which Smad4 regulates chondrocyte hypertrophy during mouse skeletal development.

Results

Deletion of Smad4 disrupts skeletal development

To investigate the role of Smad4 in limb formation, we utilized new $Tbx18^{Cre/+}$ knock-in mice (24), with which to remove Smad4 in the proximal domain of forelimbs and hindlimbs in mouse embryos (Fig. S1, *A* and *B*). To ascertain and characterize Tbx18-Cre-mediated Cre-loxP recombination during limb development, $Tbx18^{Cre/+}$ knock-in mice were crossed to $Rosa26^{nlacZ/+}$ and $Rosa26^{GFP/+}$ reporter mice (25, 26). Lineage tracing showed that Tbx18 descendants ($Tbx18^{Cre/+}$; $Rosa26^{nlacZ/+}$ and $Tbx18^{Cre/+}$;$Rosa26^{GFP/+}$) include the proximal domain of the limbs at E9.5–13.5 (Fig. S1, *C* and *D*). Further immunostaining revealed that Tbx18 lineage cells are mainly co-localized with Sox9 in chondrocytes at E12.5–13.5 (Fig. S1, *E* and *F*), suggesting $Tbx18^{Cre/+}$ lineages mark chondrocytes in the proximal domain of the limbs.

To delete Smad4 in the chondrocytes, $Tbx18^{Cre/+}$ mice were crossed to *Smad4-flox* ($Smad4^{f/f}$) (27) to obtain $Tbx18^{Cre/+}$; $Smad4^{f/+}$ compound heterozygous animals. They were further crossed to $Smad4^{f/f}$ mice to generate $Tbx18^{Cre/+}$;$Smad4^{f/f}$ mutants (denoted as *Smad4 CKO*). We found mice with the $Tbx18^{Cre/+}$;$Smad4^{f/+}$ genotype are normal and therefore utilized as controls in this study. Immunostaining revealed that Smad4 is ubiquitously expressed in the WT and $Tbx18^{Cre/+}$; $Smad4^{f/+}$ control limb at E11.5–13.5 (Fig. 1*A*, data not shown for WT). In *Smad4 CKO* embryos, almost no Smad4 expression was detected in the chondrocytes and adjacent perichondrial cells (Fig. 1*B*), suggesting that *Smad4* is removed in these regions. The mutant mice died shortly after birth with severe ureteral development defects (24). At E14.5, they displayed a prominently shortened limb (*arrows* in Fig. 1, *C* and *D*), and the defect became severe at E16.5 and E18.5 (Fig. 1, *E–J*). Further skeletal analysis by Alizarin red and Alcian blue staining showed that the limb shortening was mainly due to the absence of stylopod elements (humerus and femur, *arrows* in Fig. 1, *K–R*) that failed in ossification at E15.5–18.5, indicating the defect was associated with abnormal chondrocyte differentiation. Additionally, zeugopod elements of the mutant limb (radius/ulna and tibia/fibula, *arrowheads* in Fig. 1, *K–R*, Fig. S2) were shorter than the control littermates. Because the stylopod elements were the most severely affected in both forelimbs and hindlimbs, we focused on the stylopod elements (humerus) in the forelimbs.

Loss of Smad4 causes chondrodysplasia in limb development

To investigate the cause of the shortened limbs in *Smad4 CKO* mice, we examined younger stage embryos from E10.5 to determine when the defects first appear. No apparent abnormalities were observed at E12.5 or earlier stages in the mutant (data not shown), except that the cartilage element was slightly shorter and smaller at E12.5 (Fig. 2, *A* and *B*). The difference became significant at E13.5 (Fig. 2, *C* and *D*), and was severe at E14.5 (Fig. 2, *E* and *F*). We analyzed the expression of chondrocyte differentiation markers including *Lect1*, *Col2a1*, and *Acan* (5, 28, 29) to determine whether chondrocyte differentiation was affected in the limbs at E12.5–13.5. Compared with control humerus, lower expression levels of *Lect1* and *Col2a1* were detected in the mutant humerus by RNA *in situ* hybridization (Fig. 2, *G–L*). Quantitative RT-PCR (qRT-PCR) confirmed that *Lect1*, *Col2a1*, and *Acan* mRNA expression levels were significantly lower by 50, 55, and 58% at E12.5, and by 63, 60, and 65% in the mutant forelimbs at E13.5, respectively (Fig. 2, *M–O*). The down-regulated *Lect1*, *Col2a1*, and *Acan* expression suggests that Smad4 is essential for chondrocyte differentiation.

Smad4 is essential for chondrocyte hypertrophy

Failure of endochondral ossification in stylopod elements is the most striking defect in *Smad4 CKO* limbs at E15.5 (*arrows* in Fig. 1, *K* and *L*). Chondrocyte hypertrophy is a crucial developmental step for endochondral ossification. Lack of hypertrophic chondrocytes could cause failure of endochondral ossification (5). We then try to determine whether chondrocyte hypertrophy is perturbed in *Smad4 CKO* limb. For $Tbx18^{Cre/+}$; $Smad4^{f/+}$ and WT limb at E13.5. H&E staining showed that chondrocytes were present in the center of humerus with hypertrophic differentiation (Fig. 3*A*). These hypertrophic characteristics were unable to be detected in the *Smad4 CKO* humerus (Fig. 3*B*). At E14.5, typical hypertrophic cells were present in the control humerus (Fig. 3*C*), and they were absent in the mutants (Fig. 3*D*). Alcian blue staining further confirmed the absence of hypertrophic chondrocytes in the mutant humerus (Fig. 3, *E–H*). We next performed RNA *in situ* hybridization to detect Col10a1, a specific marker for hypertrophic chondrocytes (30, 31), and *Panx3*, a marker for prehypertrophic and hypertrophic chondrocytes (32, 33). Both *Col10a1* and

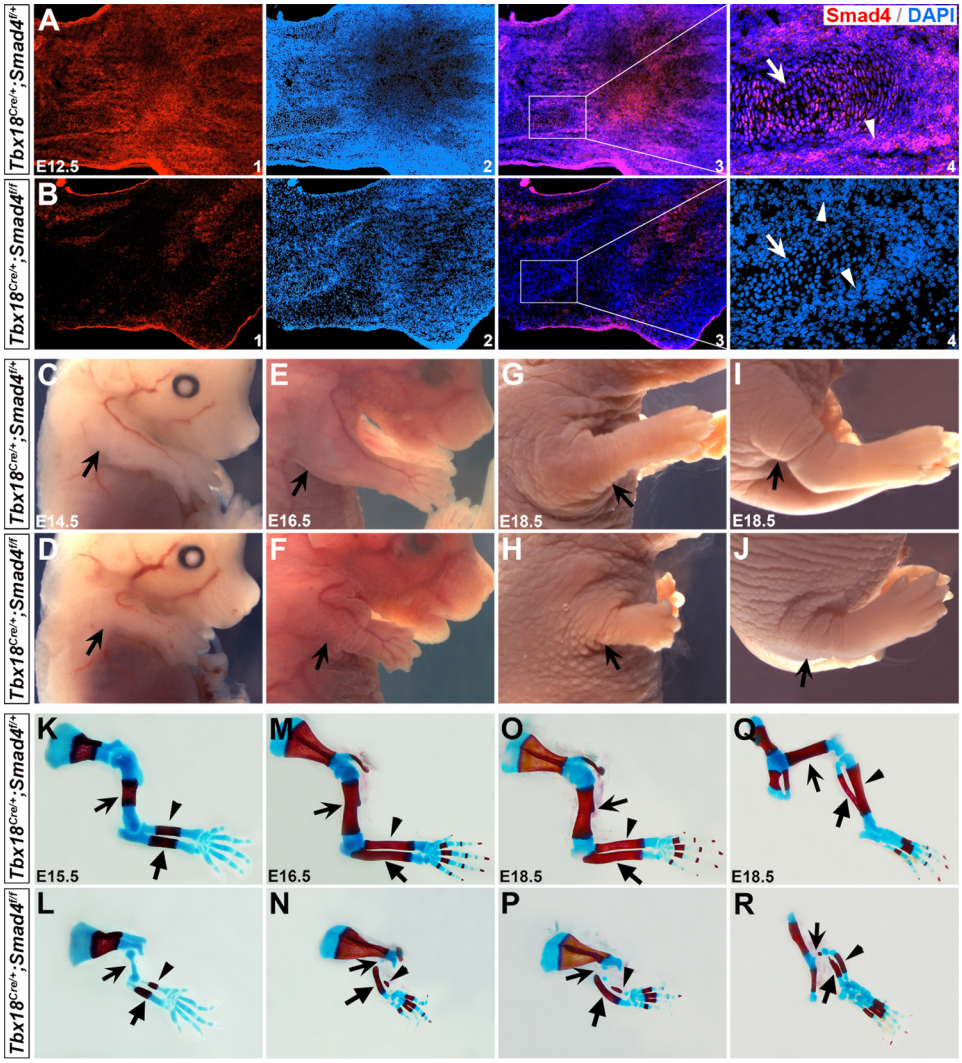

Figure 1. Impaired skeletal development in Smad4 mutant mice. *A* and *B,* immunostaining of Smad4 on the forelimb on the control and mutant mice at E12.5. *Arrows* indicate chondrocytes and *arrowheads* indicate perichondrial cells. *A3* and *B3* are overlay images for *A1/2* and *B1/2*, respectively. *A4* and *B4* are high magnification images in the areas outlined in *A3* and *B3*. *C–J,* whole mount view of *Smad4 CKO* mice at E14.5–18.5. *Arrows* indicate control forelimb (*C*, *E*, and *G*) and hindlimb (*I*), or mutant forelimb (*D*, *F*, and *H*) and hindlimb (*J*). *K–R,* skeletons of E15.5–18.5 embryos stained with Alizarin red (calcified tissue) and Alcian blue (cartilage). *K*, *M*, *O*, and *Q* are controls and *L*, *N*, *P*, and *R* are mutants. In *K–P*, *arrows*, *arrowheads*, and *unnotched arrows* indicate humerus, radius, and ulna, respectively. In *Q* and *R*, *arrows*, *arrowheads,* and *unnotched arrows* indicate femur, fibula, and tibia, respectively.

Panx3 were found in the center of humerus as early as E12.5 in the control (Fig. 3, *I* and *O*), but were undetectable in the mutant (Fig. 3, *J* and *P*). At E13.5 and E14.5, robust *Col10a1* and *Panx3* expression was detected in the hypertrophic or prehypertrophic region on the control mice (Fig. 3, *K*, *M*, *Q*, and *S*), and they were not seen in the mutant humerus (Fig. 3, *L*, *N*, *R*, and *T*). Further qRT-PCR analysis showed that *Col10a1* and *Panx3* mRNA expression was decreased by 70 and 90% at E12.5, and by 76 and 87% at E13.5 in the mutant forelimbs, respectively (Fig. 3, *U* and *V*). Taken together, these observations indicate that the primary chondrocytes of *Smad4 CKO* humerus failed to undergo hypertrophic differentiation, and Smad4 is critical for chondrocyte hypertrophy development during limb formation.

Smad4 deficiency results in decreased chondrocyte proliferation

Chondrocyte proliferation is important for cartilage growth prior to hypertrophic differentiation. Given the small humerus in the mutant limb at E12.5 and onward, we hypothesized that Smad4 signals may be essential for chondrocyte growth. To confirm this, EdU was injected into pregnant mice intraperitoneally at E12.5 and E13.5, and forelimbs were collected after 4 h of injection for analysis. The proliferating cells in the cartilage were analyzed by immunofluorescence to determine whether chondrocyte proliferation was affected in the mutants. The proliferation rate was calculated by the ratio of EdU/Sox9 double positive cells divided by the total of chondrocyte cells (Sox9 positive) in humerus. It showed that the mutant chondrocyte proliferation was significantly reduced more than that of the control, with 18.4% in the control *versus* 14.2% in the mutant at E12.5, and 17.8% in the control *versus* 13.1% in the mutant at E13.5 (Fig. 4). These results uncover that Smad4 signaling is required for chondrocyte proliferation.

Smad4 is required for Runx2 expression in the limb

To further elucidate the molecular mechanism by which *Smad4* deficiency impairs chondrocyte hypertrophy, we per-

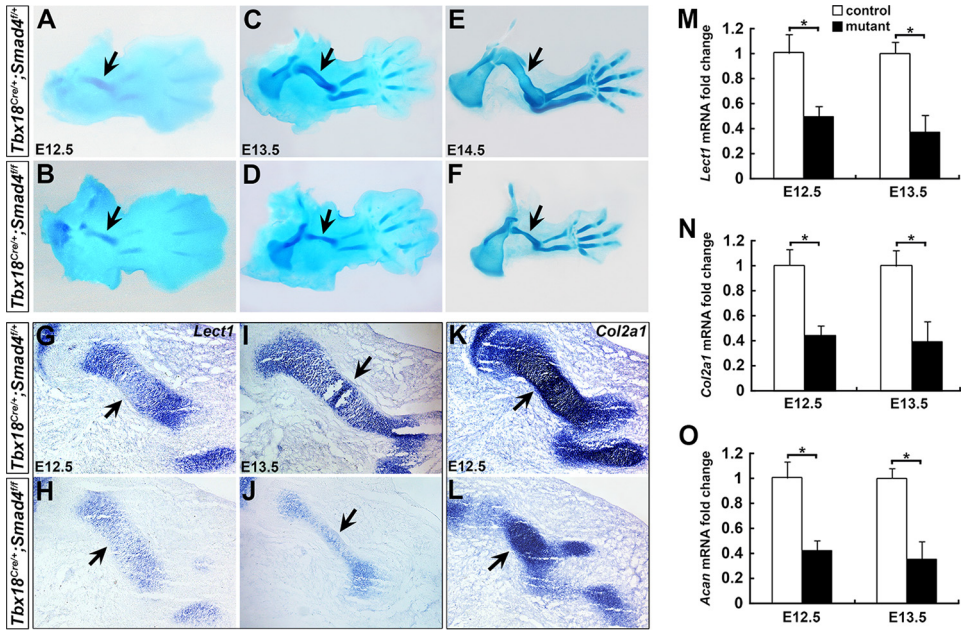

Figure 2. Chondrodysplasia in the limbs of Smad4 mutant mice. *A–F,* Alcian blue staining on the control (*A*, *C*, and *E*) and mutant forelimbs (*B*, *D*, and *F*) at E12.5–14.5. *Arrows* in *A–F* indicate humerus. *G–L,* RNA *in situ* hybridization for *Lect1* and *Col2a1* on the forelimb sections at E12.5 and E13.5. *Arrows* indicate RNA expression in humerus. *M–O*, *Lect1*, *Col2a1,* and *Acan* expression level was evaluated by qRT-PCR in the forelimbs at E12.5 and E13.5. $n = 3$, *, $p < 0.05$.

formed high-throughput RNA-seq to examine genes with altered expression when Smad4 is removed. Because *Smad4 CKO* limb defects were first detected at E12.5, and chondrocytes start the hypertrophic differentiation process at E13.5 and are largely accomplished at E14.5 (Fig. 3, *A*, *C*, *E*, and *G*), we isolated RNA at E12.5, E13.5, and E14.5 from forelimbs of mutants and controls for large-scale sequencing. Furthermore, to examine whether any molecular changes occur before E12.5, we also performed RNA-seq with E11.5 forelimb samples although no morphological abnormalities were detected.

Approximately 30 million raw reads per sample were obtained and the reads with good quality were aligned to mouse reference sequence (RefSeq) transcripts using BWA (34). In *Smad4 CKO* mice, 551 genes at E12.5 (Table S3) and 622 genes at E13.5 (Table S4) were down-regulated ($p < 0.0001$) using the DEGseq program (35), and the number increased to 2581 at E14.5 (Table S5) (Fig. 5*A*). As parallel, the number of up-regulated genes ($p < 0.0001$) was increased from 651, 775 to 3249 at E12.5 (Table S3), E13.5 (Table S4), and E14.5 (Table S5), respectively (Fig. 5*B*). At E11.5, very few genes (less than 10) were changed (Tables S7 and S8) and they seemed not associated with chondrocyte/limb development according to Gene Ontology (GO) analysis using DAVID 6.7 (36). At E12.5–14.5, the number of significantly changed genes appeared to reflect the degree of abnormalities between the mutant and control at corresponding stages (Fig. 2, *A–F*). A larger number of the overlapped genes were found between E13.5 and E14.5 (Tables S11 and S12) than E12.5 and E14.5 (Tables S13 and S14) or E12.5 and E13.5 (Tables S9 and S10) (Fig. 5, *A* and *B*). In addition, 123 genes were down-regulated (Table S15, Fig. 5*A*) and 30 genes were up-regulated (Table S16, Fig. 5*B*) at all three stages. At E12.5, the down-regulated genes are highly associated with skeletal, cartilage, and bone development (*asterisks* in Fig. 5*C*, and Tables S17 and S18). At E13.5, skeletal, cartilage, and limb/bone development are still on the top lists of term according to GO (*asterisks* in Fig. 5*D*, Tables S19 and S20). It is of importance to note that although many genes were changed at E14.5, the limb/bone, skeletal, and cartilage development are not the primary terms (Tables S21 and S22). This may suggest that the genes changed at E14.5 are secondary or may not be directly regulated by Smad4.

Of interest, we found the down-regulated genes at E12.5 and E13.5, including *Acan*, *Col10a1*, *Col2a1*, *Fgfr3*, *Ihh*, *Lect1*, *Runx2*, *Runx3*, and *Sp7*, are highly related to chondrocyte differentiation and hypertrophy (Fig. 5*E*) (11, 15, 28, 30, 37–40). In agreement with RNA-Seq analysis, qRT-PCR further confirmed that expression of *Runx2*, *Runx3*, *Ihh,* and *Sp7* was reduced by 42, 40, 41, and 58% at E12.5, and 53, 45, 55, and 59% at E13.5 in the mutant, respectively (Fig. 6*Q*). We performed immunofluorescence and RNA *in situ* hybridization to examine expression of these genes. It showed that *Runx2*, *Runx3*, *Ihh*, and *Sp7* were dramatically down-regulated in *Smad4*-deficient humerus (E12.5–13.5, Fig. 6, *A–P*), suggesting Runx2, Runx3, Ihh, and Sp7 may regulate hypertrophic chondrocyte differentiation as downstream of Smad4.

Smad4 directly binds to Runx2 regulatory elements

RNA-seq analysis of *Smad4 CKO* forelimb revealed that most genes remain normal at E11.5, and the genes with altered expression at E14.5 are likely secondary and may not reflect direct regulation by Smad4 during limb development. We next performed ChIP-seq with E12.5 and E13.5 forelimbs to determine Smad4 direct downstream targets in chondrocyte hypertrophy development. Chromatin DNA was prepared from the WT forelimb tissues at E12.5 and E13.5 using anti-Smad4 antibody. The purified DNA was amplified for library construction and large-scale sequencing. Smad4 genome-wide occupancy was identified using MACS1.4 as described (41). Peaks within 5

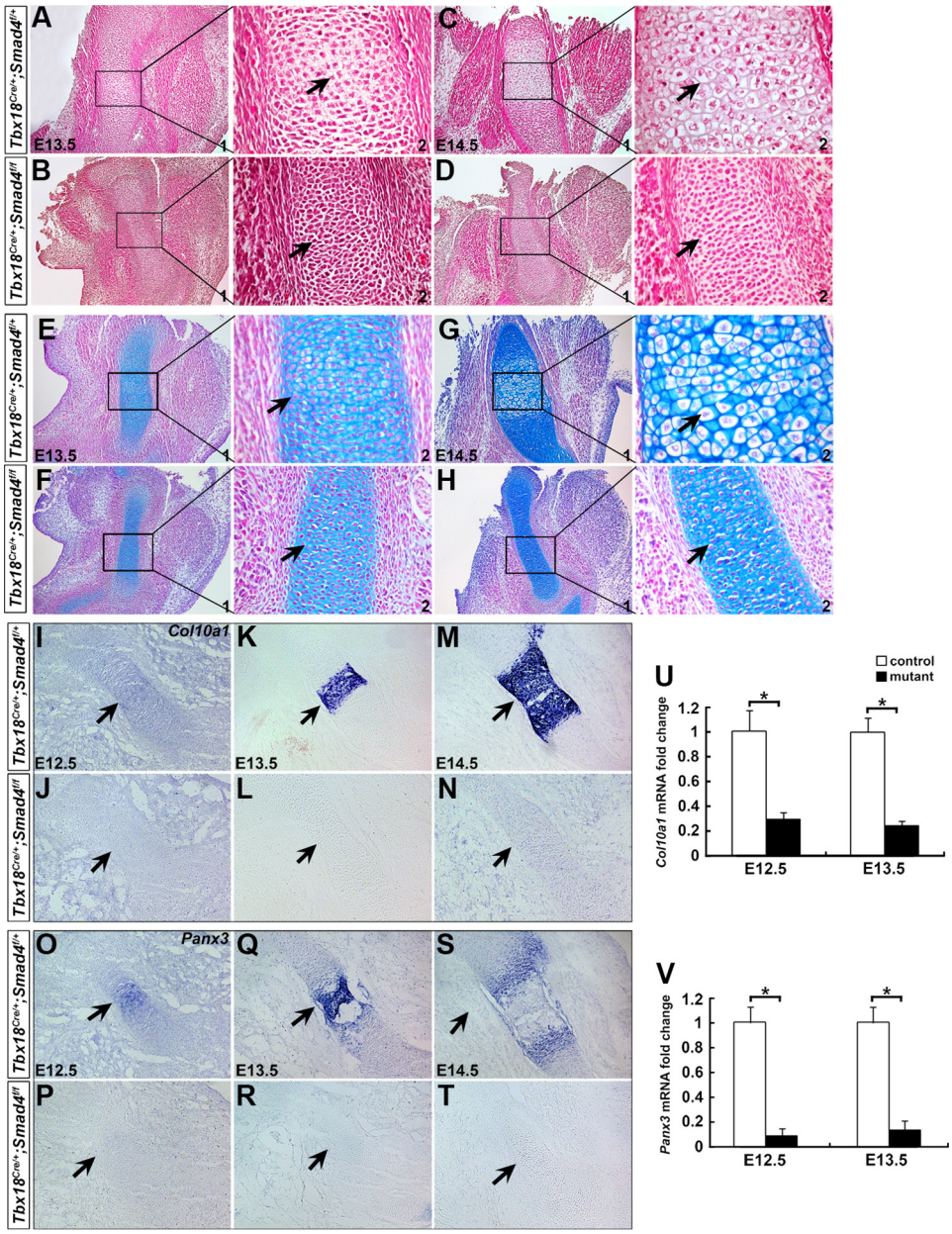

Figure 3. Lack of chondrocyte hypertrophy in *Smad4 CKO* humerus. *A–H,* H&E and Alcian blue staining on the control and mutant forelimbs at E13.5 and 14.5. *A2–H2* are magnified images for *A1–H1* showing chondrocytes (*arrows*) in the humerus. Hypertrophic chondrocytes were observed in the control humerus (*arrows* in *C2* and *G2*), but not in the mutant (*arrows* in *D2* and *H2*) at E14.5. *I–T,* section RNA *in situ* hybridization for *Col10a1* and *Panx3* on the forelimb at E12.5–14.5. *Arrows* indicate RNA expression in humerus. *U* and *V, Col10a1* and *Panx3* expression in the forelimbs was determined by qRT-PCR at E12.5 and E13.5. $n = 3$, *, $p < 0.01$.

kb of the transcription start site (TSS) were assigned to the nearest genes. Regulatory regions in 1213 genes were identified and potentially bound by Smad4 (Table S6). We performed GO analysis on these genes and found that *regulation of chondrocyte differentiation* was on the top of the list (*asterisk* in Fig. 7*B*, Table S23).

To determine whether Smad4 directly regulated genes are associated with chondrocyte differentiation, we combined RNA-seq and ChIP-seq data (E12.5–13.5) for further integrative analysis. It revealed that 6 down-regulated genes, including *Runx2* and *Fgfr3*, are related to cartilage development (Fig. 7*A*, see full list of the genes in Table S24). In contrast, the up-regulated 4 genes seem not to be associated with chondrocyte differentiation (Fig. 7*A*, Table S25). Consensus core sequences 5′-GTCT-3′ were called and are consistent with previously reported Smad-binding elements (42, 43). Because the Smad4 binding motif is already known in HOMER database (http://homer.ucsd.edu/homer/motif/motifDatabase.html)[4] (Fig. 7, *C-1*), we applied HOMER motif discovery software (44) to screen for all enriched regions, and found the Smad4-binding motif (5′-TTTTGTCTGC-3′) is in the list of enrichment peaks (Fig. 7, *C-2*). The Smad4-enrichment peak in *Runx2* is ~4 kb upstream of TSS (two Smad-binding elements within the

[4] Please note that the JBC is not responsible for the long-term archiving and maintenance of this site or any other third party hosted site.

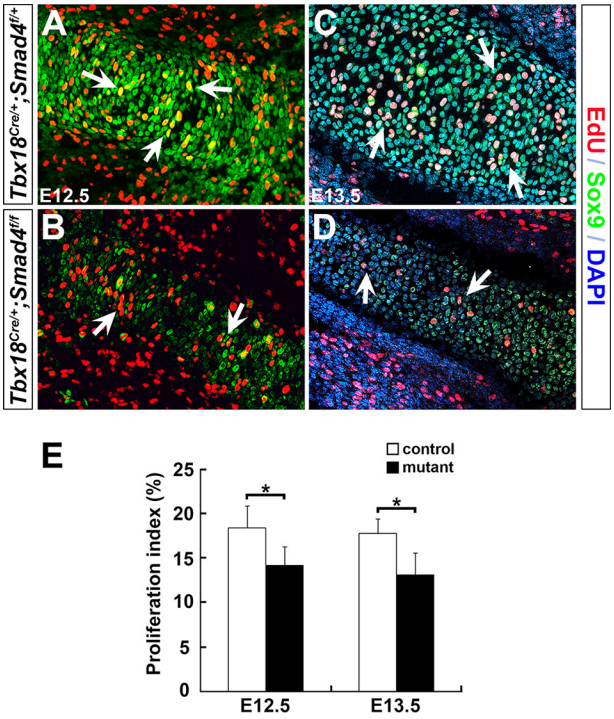

Figure 4. Decreased chondrocyte proliferation in Smad4 mutant mice. *A–D,* chondrocyte proliferation was analyzed by EdU labeling (*red*). Sox9 (*green*) was used to mark chondrocytes. *Arrows* indicate EdU-positive chondrocytes. *E,* EdU-positive cells were quantified. The proliferation rate of chondrocytes was represented by the ratio of EdU/Sox9 double positive cells normalized to Sox9 positive cells in humerus. $n = 3$, *, $p < 0.05$.

enriched peak), and the motif is 76 bp away from the peak midpoint. The Integrative Genomics Viewer (45) peak upstream of *Runx2* TSS was shown in Fig. 7*C*. To verify direct binding of the *Runx2* regulatory element by Smad4, we further carried out ChIP-PCR around this region with chromatin DNA immunoprecipitated by Smad4 antibody in mouse forelimbs (E12.5–13.5), with DNA ChIPed by IgG as control. The *Runx2* regulatory region containing the Smad4-binding site was amplified by PCR (Fig. 7*D*), confirming that Smad4 directly binds to this *Runx2* regulatory element during mouse skeletal development at E12.5–13.5. Furthermore, luciferase reporter assays revealed that Smad4 activates the Runx2 promoter fragment containing the Smad4-binding site (5.0 kb), but not fragments without this site (4.2 and 3.0 kb) (Fig. 7*E*). Taken together, these data suggest that Smad4 directly binds to Runx2 regulatory elements during mouse limb development.

Discussion

Chondrocyte hypertrophic differentiation is a precisely regulated morphogenetic process in which the chondrocytes differentiate into hypertrophic chondrocytes during skeletal development (Fig. 8). Smad4 has been shown to play important roles in the process of chondrocyte differentiation from mesenchymal cells and chondrocyte proliferation (19, 20). In this study, we showed that Smad4 is essential for chondrocyte hypertrophic differentiation. *Smad4 CKO* mice display limb growth defects with chondrodysplasia characterized by low chondrocyte proliferation and lack of hypertrophy in humerus. We further demonstrated that Smad4 acts as a direct transcriptional activator for *Runx2* in chondrocyte differentiation.

Smad4 regulates chondrocyte differentiation and hypertrophy

Previous studies showed that ablation of *Smad4* with *Prx1-Cre* or *Col2a1-Cre* deleter mice resulted in defective limb formation (19, 20). Specifically, *Prx1-Cre;Smad4$^{f/f}$* mutant mice displayed a complete loss of limb skeletal elements at E14.5 due to perturbation of mesenchymal cell aggregation, the first step of chondrocyte differentiation (20). *Col2a1-Cre;Smad4$^{f/f}$* mutant mice displayed a mild shortened limb at postnatal day 10 with defective proliferation and differentiation of chondrocytes (19). In contrast to defects of these two mutants, limb shortening of *Tbx18$^{Cre/+}$;Smad4$^{f/f}$* mice resulted from the absence of stylopod elements because of chondrocyte hypertrophy failure, the terminal step of chondrocyte differentiation. Phenotype variations of these mutants could be explained by location and timing of distinct Cre-mediated genetic deletions in the developing limbs: *Prx1-Cre* is expressed in the early limb mesenchyme at E9.5 and it introduces genetic deletions in both chondrocytes and perichondrium (46). *Col2a1-Cre* is expressed in the differentiating chondrocytes in limbs (47). *Tbx18$^{Cre/+}$* is detected in the limb bud as early as E9.5 and mediates recombination in chondrocytes within the proximal domain of the limb (Fig. S1, *C–F*). The divergent defects of *Smad4* mutants suggest multiple and temporospatially distinct functions of Smad4 in limb formation.

In *Smad4 CKO* embryos, chondrocyte differentiation is severely perturbed. Cartilage elements (humerus) in the mutant limb were shorter and smaller (Fig. 2, *A–F*) with decreased *Col2a1*, *Acan*, and *Lect1* expression (Fig. 2, *G–Q*). The RNA-seq assay also showed down-regulated *Sox9*, *Sox5*, and *Sox6* (Fig. 5*E*). These genes are key transcription factors for chondrocyte differentiation (48–51). Disruption of *Sox9* leads to impaired chondrocyte differentiation and endochondral bone formation (50, 52). It was shown that Sox9 directly regulates *Col2a1* and *Acan* and promotes differentiation of mesenchymal cells to chondrocytes (38, 53, 54). Smad4 may activate *Col2a1* and *Acan* via Sox9 during chondrocyte development and this conception needs to be further determined.

Chondrocyte hypertrophy is critical for endochondral ossification. Disruption of *Smad4* in *Tbx18$^{Cre/+}$* lineage results in complete loss of chondrocyte hypertrophy (Fig. 3, *A–H*) and failure of endochondral ossification in humerus (Fig. 1, *K* and *L*), suggesting an essential role of Smad4 for chondrocyte hypertrophy during long bone development. This notion was supported by the observation of the absent hypertrophic chondrocytes and missing expression of *Col10a1* (specific marker for hypertrophic chondrocytes (30, 31)) and *Panx3* (specific marker for pre-hypertrophic chondrocytes and hypertrophic chondrocytes (32, 33)) in *Smad4 CKO* humerus (Fig. 3, *I–V*).

Runx2 acts as a crucial mediator of Smad4 signaling in chondrocyte hypertrophy

In this study, we applied RNA-seq and ChIP-seq to decipher how Smad4 controls chondrocyte hypertrophy during mouse limb skeletogenesis. GO analysis of the RNA-seq data showed the down-regulated genes are highly associated with skeletal, cartilage, and bone development at E12.5 and E13.5 (Fig. 5, *C* and *D*). RNA-seq revealed that the down-regulated genes at

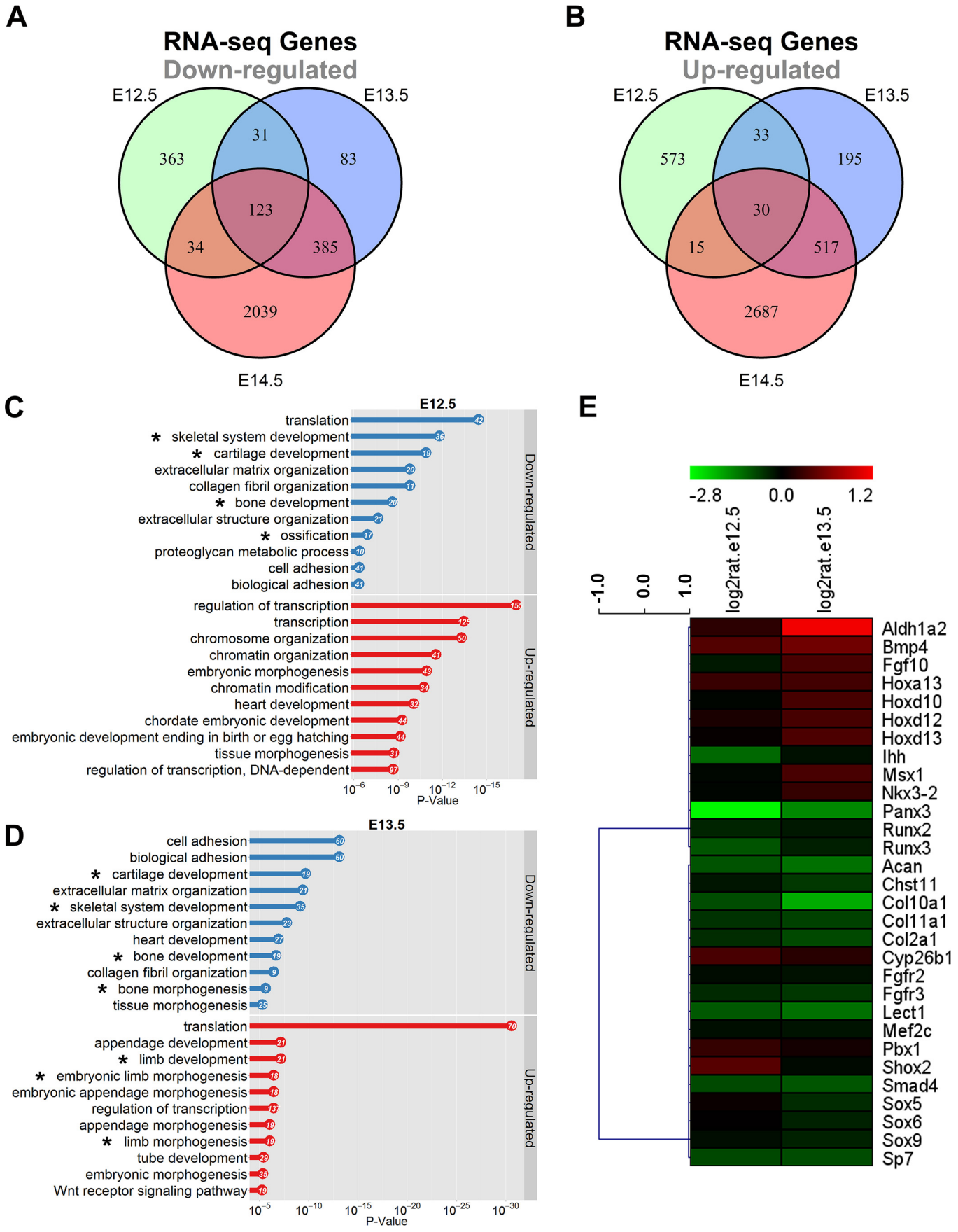
A
RNA-seq Genes
Down-regulated
E12.5
E13.5
E14.5
363
31
83
123
34
385
2039
B
RNA-seq Genes
Up-regulated
E12.5
E13.5
E14.5
573
33
195
30
15
517
2687
C
E12.5
translation
* skeletal system development
* cartilage development
extracellular matrix organization
collagen fibril organization
* bone development
extracellular structure organization
* ossification
proteoglycan metabolic process
cell adhesion
biological adhesion
regulation of transcription
transcription
chromosome organization
chromatin organization
embryonic morphogenesis
chromatin modification
heart development
chordate embryonic development
embryonic development ending in birth or egg hatching
tissue morphogenesis
regulation of transcription, DNA-dependent
Down-regulated
Up-regulated
P-Value
D
E13.5
cell adhesion
biological adhesion
* cartilage development
extracellular matrix organization
* skeletal system development
extracellular structure organization
heart development
* bone development
collagen fibril organization
* bone morphogenesis
tissue morphogenesis
translation
appendage development
* limb development
* embryonic limb morphogenesis
embryonic appendage morphogenesis
regulation of transcription
appendage morphogenesis
* limb morphogenesis
tube development
embryonic morphogenesis
Wnt receptor signaling pathway
Down-regulated
Up-regulated
P-Value
E
-2.8
0.0
1.2
-1.0
0.0
1.0
log2rat.e12.5
log2rat.e13.5
Aldh1a2
Bmp4
Fgf10
Hoxa13
Hoxd10
Hoxd12
Hoxd13
Ihh
Msx1
Nkx3-2
Panx3
Runx2
Runx3
Acan
Chst11
Col10a1
Col11a1
Col2a1
Cyp26b1
Fgfr2
Fgfr3
Lect1
Mef2c
Pbx1
Shox2
Smad4
Sox5
Sox6
Sox9
Sp7

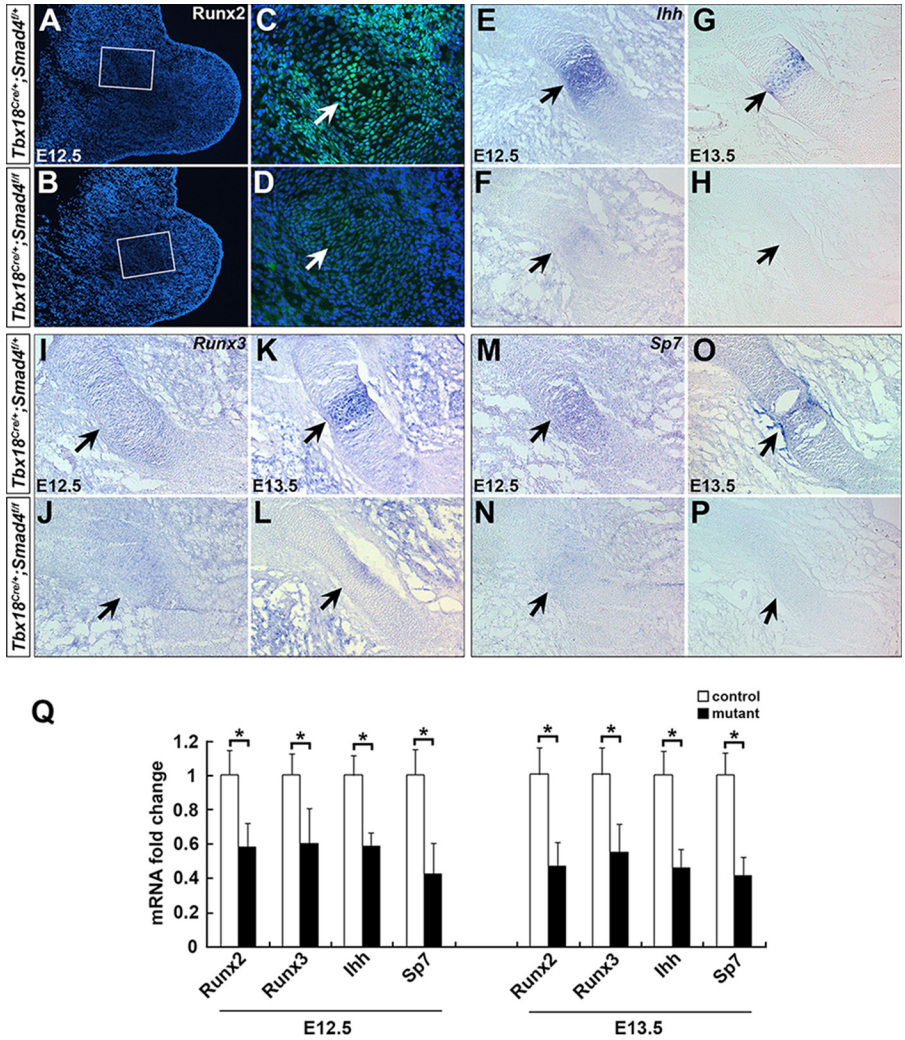

Figure 6. Reduced expression of chondrocyte hypertrophy–related genes on *Smad4* mutant mice. *A–D,* immunostaining of *Runx2* on the forelimb sections from the control (*A* and *C*) and mutant (*B* and *D*) embryos at E12.5. *E–P,* RNA *in situ* hybridization staining of *Ihh*, *Runx3*, and *Sp7* on forelimb sections from control (*E*, *G*, *I*, *K*, *M*, and *O*) and mutant (*F*, *H*, *J*, *L*, *N*, and *P*) embryos at E12.5 and E13.5. *Arrows* in *A–P* indicate protein or RNA expression in humerus. *Q, Runx2, Runx3, Ihh*, and *Sp7* RNA expression levels were determined by qRT-PCR at E12.5 and E13.5 in the forelimbs. $n = 3$, *, $p < 0.05$.

E12.5 and E13.5 included *Col10a1*, *Fgfr3*, *Ihh*, *Runx2*, *Runx3*, and *Sp7* in *Smad4 CKO* mice. These down-regulated genes are highly related to chondrocyte hypertrophy. qRT-PCR and immunofluorescence verified these genes (Figs. 3 and 6). Runx2 is a critical mediator of chondrocyte hypertrophy (16, 55–57) and it is expressed in prehypertrophic and hypertrophic chondrocytes during skeletal development. Inactivation of *Runx2* causes the absence of ossification and hypertrophic chondrocytes (16, 55, 58, 59), similar to *Smad4 CKO* mice. Col10a1 is a specific marker for hypertrophic chondrocytes, and Runx2 directly regulates the transcriptional activity of *Col10a1* (30, 31). *Ihh*, a direct target gene of Runx2, is expressed in prehypertrophic chondrocytes and is essential for chondrocyte hypertrophy (10, 11, 15). Sp7 is a zinc finger transcription factor regulating bone formation at the hypertrophic stage *in vivo* (40). Runx2 specifically binds to the regulatory element on *Sp7* promoter (60). Collectively, *Runx2*, *Runx3*, *Col10a1*, *Fgfr3*, *Ihh*, and *Sp7* may act as key downstream genes of Smad4 signaling involved in chondrocyte hypertrophy.

The integrated RNA-seq and ChIP-seq data analyses identified potential targets of Smad4. Six down-regulated genes highly related to bone formation, including *Runx2* and *Fgfr3*, were uncovered (55, 61). Fgfr3 is a negative regulator for bone growth (61). Fgfr3 was shown to restrain chondrocyte proliferation and limit osteogenesis. $Fgfr3^{-/-}$ mutant mice displayed prolonged endochondral bone growth accompanied by expansion of proliferating and hypertrophic chondrocytes in the cartilaginous growth plate. Given that Fgfr3 controls endochondral ossification by a negative regulatory mechanism, and $Fgfr3^{-/-}$ bones display prolonged defects compared with

Figure 5. Ablation of Smad4 in the forelimb causes severe impaired chondrocyte differentiation through RNA-seq analysis. *A* and *B*, the Venn diagrams showing the number of overlapping genes down-regulated (*A*) and up-regulated (*B*) in $Tbx18^{Cre/+};Smad4^{f/f}$ forelimb between E12.5, E13.5, and E14.5. Top biological process GO terms were determined using DAVID for differentially expressed genes in forelimbs at E12.5 (*C*) and E13.5 (*D*). X-axis is the *p* value for the enrichment of a GO term in the input gene list compared with genes in the whole genome. The gene numbers are listed in the *dots*. *E,* heat map of cartilage development at E12.5 and E13.5. *Red* and *green* denote up-regulated and down-regulated genes, respectively.

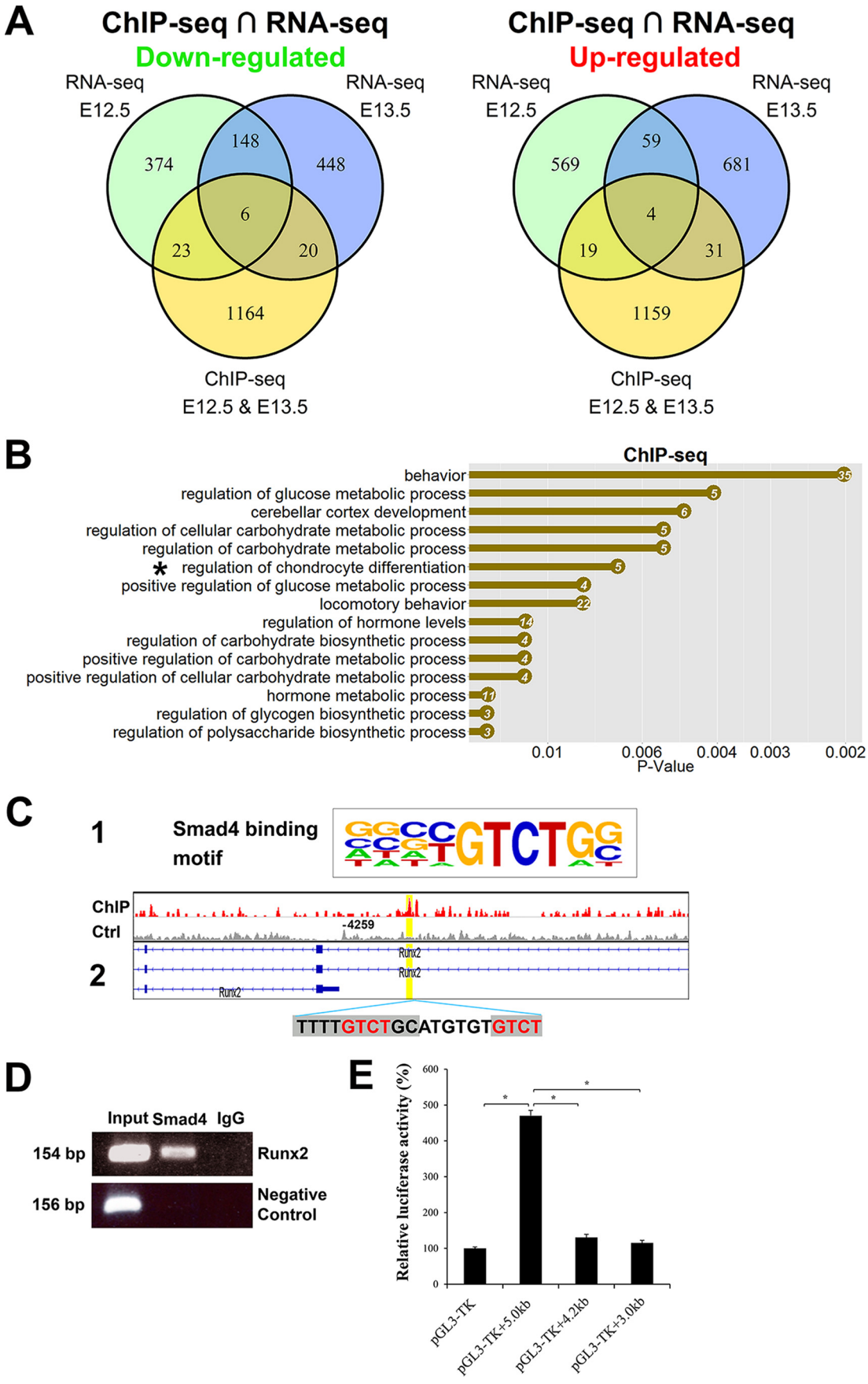
A
ChIP-seq ∩ RNA-seq
Down-regulated
RNA-seq E12.5
RNA-seq E13.5
ChIP-seq E12.5 & E13.5
374
148
448
6
23
20
1164
ChIP-seq ∩ RNA-seq
Up-regulated
RNA-seq E12.5
RNA-seq E13.5
ChIP-seq E12.5 & E13.5
569
59
681
4
19
31
1159
B
ChIP-seq
behavior
regulation of glucose metabolic process
cerebellar cortex development
regulation of cellular carbohydrate metabolic process
regulation of carbohydrate metabolic process
* regulation of chondrocyte differentiation
positive regulation of glucose metabolic process
locomotory behavior
regulation of hormone levels
regulation of carbohydrate biosynthetic process
positive regulation of carbohydrate metabolic process
positive regulation of cellular carbohydrate metabolic process
hormone metabolic process
regulation of glycogen biosynthetic process
regulation of polysaccharide biosynthetic process
35
5
6
5
5
5
4
22
14
4
4
4
11
3
3
0.01
0.006
0.004
0.003
0.002
P-Value
C
1
Smad4 binding motif
ChIP
Ctrl
-4259
2
Runx2
Runx2
Runx2
TTTTGTCTGCATGTGTGTCT
D
Input Smad4 IgG
154 bp
Runx2
156 bp
Negative Control
E
Relative luciferase activity (%)
600
500
400
300
200
100
0
*
*
*
pGL3-TK
pGL3-TK+5.0kb
pGL3-TK+4.2kb
pGL3-TK+3.0kb

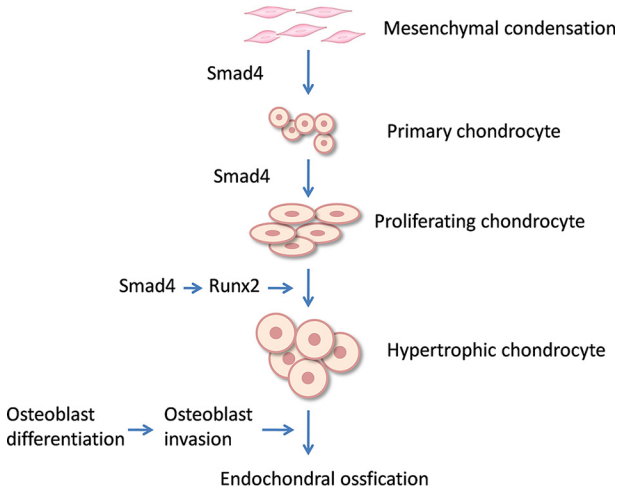

Figure 8. A model for the role of Smad4 in chondrocyte hypertrophy and bone development. Smad4 regulates chondrocyte differentiation and proliferation. Runx2 is required for chondrocyte hypertrophic differentiation. Smad4 controls chondrocyte hypertrophy and bone development through regulation of Runx2.

Smad4 CKO mice (Fig. 1, *K–R*), the down-regulated *Fgfr3* may not be the main cause of *Smad4 CKO* limb defects, although Smad4/Fgfr3 signaling cascade could play some unknown essential roles for limb skeletal development. In contrast, Runx2 positively regulates chondrocyte hypertrophy. Runx2 overexpression in chondrocytes restores chondrocyte hypertrophy in *Runx2*-deficient mice (56, 57). Taken together, our data support that *Runx2* acts as a key downstream gene of Smad4 given the critical role of Runx2 in the skeletal hypertrophic development.

Runx2 has been suggested as a common downstream gene of TGF-β/BMP signaling in previous studies, although the mechanisms underlying this process were largely unknown before (22, 62). In this regard, our study first demonstrated that Smad4 transcriptionally activates *Runx2* expression by directly binding to *Runx2* regulatory elements during chondrocyte hypertrophy, suggesting an important role of Runx2 in cartilage growth and bone formation.

Smad4 is required for chondrocyte proliferation

Chondrocyte proliferation is essential for cartilage growth (11, 63, 64). BMP signaling was shown to be important for chondrocyte proliferation (14, 65). Reduced osteoblast and chondrocyte proliferation was detected in *Smad4* mutant mice in the previous studies (18, 19). Here we found that ablation of *Smad4* with $Tbx18^{Cre/+}$ also led to a dramatic reduction in chondrocyte proliferation as early as E12.5 in the forelimb (humerus). The reduced chondrocyte proliferation should contribute to the short cartilage elements in *Smad4 CKO* limbs (Fig. 2, *A–F*). Smad4 promotes *Ihh* expression (Figs. 5*E* and 6, *E–H* and *Q*), and Ihh plays a critical role in regulating chondrocyte proliferation during skeletal development (11, 64, 66). *Ihh*-deficient mice display severe reduction in skeletal growth and decreased chondrocyte proliferation (11). Ectopic activation of Ihh signaling promotes chondrocyte proliferation during cartilage development (64). Given that *Ihh* was significantly down-regulated in *Smad4 CKO* humerus, it is potential that Ihh is one of the key downstream effectors of Smad4 signaling pathways in regulating chondrocyte proliferation.

In summary, our study uncovered divergent, crucial roles of Smad4 in chondrocyte differentiation, especially in hypertrophic differentiation during limb development. We demonstrated that Smad4 controls chondrocyte hypertrophic differentiation through direct regulation of *Runx2*. Ablation of *Smad4* within the proximal domain of limbs results in chondrodysplasia due to reduced chondrocyte proliferation, impaired chondrocyte differentiation, lack of chondrocyte hypertrophy, and failure of ossification in humerus. As the study did not use hypertrophic chondrocyte-specific Cre (*e.g. Col10a-Cre*) to delete Smad4 from hypertrophic chondrocytes in the limb, it is uncertain whether the impaired chondrogenesis also affects chondrocyte hypertrophy in *Smad4 CKO* mice. ChIP-seq assay uncovered a previously unknown critical role of *Runx2* as a direct downstream target of Smad4 signaling in cartilage and bone formation. The Smad4–Runx2 regulatory pathways provide important mechanisms to understand hypertrophic differentiation of limb development and etiology of chondrodysplasia in mammals.

Experimental procedures

Animals

All animal experiments conformed to the United States National Institutes of Health guidelines and were conducted in accordance with the protocol approved by the Institutional Animal Care and Use Committee (IACUC) at Icahn School of Medicine at Mount Sinai (Permit LA09-00494). *Smad4-floxed* (denoted as $Smad4^{f/f}$), *Rosa26:lacZ* ($Rosa26^{lacZ/+}$), *Rosa26:GFP* ($Rosa26^{GFP/+}$), *Tbx18:Cre* ($Tbx18^{Cre/+}$), and *Tbx18:nlacZ* ($Tbx18^{nlacZ/+}$) mice were described previously (24–27, 67). Mouse tails or yolk sac tissues were collected for genotyping.

Skeletal analysis

Calcified tissue was stained with Alizarin red (Sigma) and cartilage was stained with Alcian blue (Sigma) with a standard procedure (68). For E15.5–18.5 embryos, the skin and internal organs were removed. Skeletons were fixed in 95% ethanol overnight and stained with 0.015% Alcian blue followed by digestion in 1% potassium chloride for 2 days, and then stained

Figure 7. Genomewide Smad4-binding sites are associated with chondrocyte differentiation. *A,* Venn diagrams show the number of down-regulated and up-regulated overlapping genes in E12.5 and E13.5 forelimbs analyzed by ChIP-seq and RNA-seq. *B,* top biological process GO terms were determined by DAVID in Smad4-binding genes. *X* axis is the *p* value for the enrichment of a GO term in the input gene list compared with genes in the whole genome. The number of genes is listed in the *dots*. *C-1,* Smad4-binding motif in the HOMER database. *C-2,* ChIP-seq analysis shows Smad4-binding site on the *Runx2*-regulatory region (binding motif was marked by *gray* and core sequence was labeled by *red*). *D,* ChIP-PCR verification of Smad4 binding on the *Runx2*-regulatory region. ChIP was performed anti-Smad4 antibody. A positive band was amplified using primers spanning the Smad4-binding site in the *Runx2* promoter with input DNA (*lane 1*) and Smad4-ChIPed DNA (*lane 2*), but was not amplified with template ChIPed by IgG (*lane 3*). Negative control is PCR with *GAPDH-CNAP1* primers. *E,* luciferase reporter assays of the Smad4 expression vector with various Runx2 promoter fragments. The putative Smad4-binding site is present in the 5.0-kb fragment, but not in the 3.0- and 4.2-kb fragments. *, $p < 0.01$.

with 0.005% Alizarin red for 3 days. E12.5–14.5 embryos were fixed in ethanol overnight, stained with 0.009% Alcian blue for 3 days, and cleared by benzyl alcohol/benzyl benzoate. Images of the stained skeletons and cartilages were taken under a Leica stereomicroscope.

X-Gal staining

Embryos were fixed with 4% paraformaldehyde (PFA) for 30 min at 4 °C. The fixed embryos were washed twice with PBS and then stained with X-Gal staining solution (5 mM potassium ferricyanide, 5 mM potassium ferrocyanide, 2 mM $MgCl_2$, 1 mg/ml X-Gal) for 12 h at room temperature.

H&E staining and Alcian blue staining

Mouse embryos were fixed with 4% PFA overnight at 4 °C and then dehydrated in an ascending ethanol series followed by two changes of 100% xylene. The tissues were embedded in liquid paraffin and placed on a cold plate for solidification. Sections were cut into 6-μm thickness on a microtome and stained with hematoxylin and eosin (H&E). For Alcian blue staining, the sections were stained in 1% Alcian blue solution (in 3% acetic acid) for 20 min and counterstained in nuclear fast red solution (Eng Scientific) for 10 min.

Immunofluorescence

Mouse limbs were fixed in 4% PFA for 30 min and embedded in Optimal Cutting Temperature compound (Tissue-Tek). Frozen samples were cut into 6-μm thickness. Sections were incubated for specific primary antibodies for 1 h at room temperature. The primary antibodies used in this study were: rabbit anti-Smad4 (1:100, Millipore), rabbit anti-Sox9 (1:300, Millipore), and mouse anti-Runx2 (1:200, Abcam). Alexa Fluor 488- or 594-conjugated secondary antibodies (1:500; Invitrogen) were used to detect the corresponding primary antibodies. Sections were then counterstained with 4′,6-diamidino-2-phenylindole, and examined by fluorescence.

RNA in situ hybridization

Whole mount and section RNA *in situ* hybridization was performed as described previously (69). *Col2a1*, *Col10a1*, *Ihh*, and *Runx3* probes were obtained from Dr. John Cobb (University of Calgary, Canada). *Fgf4*, *Fgf8, Shh, Hoxa13, and Hoxd11* probes were from Dr. Brian Harfe (University of Florida). *Ezh2, Hoxa11, Hand2, and Gli3* probes were from Dr. Sevan Hopyan (University of Toronto, Canada). *Fgf10* probe was obtained from Dr. Juan Jose Sanz-Ezquerro (National Center for Biotechnology, Spain). *Raldh2* probe was from Dr. Gregg Duester (Sanford-Burnham Medical Research Institute) and the *Cyp26b1* probe was from Dr. Martin Petkovich (Queen's University, Canada). *Chondromodulin 1 (Lect1)*, *Osterix* (*Sp7*), and *Pannexin 3* (*Panx3*) cDNA fragments were generated by RT-PCR. Antisense probes were synthesized with RNA polymerases (Promega) and DIG RNA Labeling Mix (Roche Applied Science). Primer sequences for RNA probes are listed in Table S1.

Cell proliferation assay

Click-iT EdU Cell Proliferation Assay Kit (Invitrogen) was used for the cell proliferation assay according to the manufacturer's instructions. Pregnant mice were intraperitoneally injected with 10 mM EdU in PBS (5 mg/100 g body weight). Embryos were collected 4 h after EdU injection and fixed with 4% PFA for 30 min at 4 °C and washed with PBS twice. Samples were embedded in Optimal Cutting Temperature compound and sectioned into 6 μm pieces. Frozen sections were incubated with Click-iT Reaction mixture for 30 min at room temperature. Slides were analyzed under a fluorescence microscope.

qRT-PCR

Total RNA was isolated from the forelimbs of mouse embryos using TRIzol reagent (Invitrogen). First strand cDNA was synthesized with QuantiTect Reverse Transcription Kit (Qiagen). qRT-PCR was carried out using the StepOne Plus PCR system (Applied Biosystems) and SYBR Green (Qiagen). The mRNA expression level was normalized to β-actin. Statistical analysis was performed by t test and $p < 0.05$ was considered significant. Primer sequences for qRT-PCR are listed in Table S2.

RNA-Seq (RNA-seq)

Total RNA was prepared using TRIzol reagent (Invitrogen) and RNA quality was determined using an Agilent Bioanalyser. RNA-seq Sample Preparation Kit (Illumina) was used to prepare mRNA and cDNA following the manufacturer's protocol. RNA-Seq (RNA-seq) was performed as described previously using a HiSeq 2500 (Illumina) (69).

ChIP-seq and ChIP-PCR

Mouse forelimbs at E12.5 and E13.5 were collected in ice-cold PBS and cross-linked immediately in 1% formaldehyde, PBS at room temperature for 15 min. The forelimbs were washed twice with PBS, and then crushed in Lysis Buffer (50 mM HEPES, pH 8.0, 140 mM NaCl, 1 mM EDTA, 10% glycerol, 0.5% IGEPAL-CA630, 0.25% Triton X-100) with 1 mM PMSF and protease inhibitor mixture (Roche Applied Science) on a Benchmark BeadBug Homogenizer. The chromatin was resuspended in the Shearing Buffer (0.1% SDS, 1 mM EDTA, 10 mM Tris-HCl, pH 8.0) and sonicated to 100–300 bp by a Covaris S220 Focused ultrasonicator. Dynabeads® Magnetic Protein A and G beads (Invitrogen) were pre-blocked with SEA BLOCK Blocking Buffer (Thermo), and the chromatin was pre-cleared with Protein A and G beads. Smad4 ChIP was performed using anti-rabbit Smad4 antibody (04-1033, Millipore) and IgG control antibody (ab136636, Abcam). In brief, 10 μl of Protein A and 10 μl of Protein G beads were incubated with 1 ml of sheared chromatin and 10 μl of antibody overnight at 4 °C. The beads were then washed once with Low Salt Wash Buffer (2 mM EDTA, 20 mM HEPES, pH 8.0, 150 mM NaCl, 0.1% SDS, 1% Triton X-100), High Salt Wash Buffer (2 mM EDTA, 20 mM HEPES, pH 8.0, 500 mM NaCl, 0.1% SDS, 1% Triton X-100), and LiCl Wash Buffer (250 mM LiCl, 1% IGEPAL-CA630, 1% deoxycholic acid sodium salt, 1 mM EDTA, 10 mM Tris, pH 8.0), respectively. The beads were eluted in 100 μl of Elution Buffer (20 mM Tris-HCl, pH 7.5, 5 mM EDTA, 50 mM NaCl, 1% SDS). Chromatin DNA was reverse cross-linked by adding 1 μl of Proteinase K (20 mg/ml) and incubation at 65 °C for 4 h. DNA sample was purified by Qiagen MinElute PCR Purification Kit,

and was amplified with an Illumina ChIP-seq DNA Sample Prep Kit (IP-102-1001). DNA libraries were sent for sequencing with an Illumina HiSeq 2500 sequencer. ChIP-PCR was performed as described previously (69). Primers used for ChIP-PCR are listed in Table S1.

Luciferase reporter assay

ATDC5 cells were transfected with a mixture of luciferase reporter plasmid containing Runx2 promoter fragments (200 ng), Smad4 expression vector (200 ng), and *Renilla* plasmid (5 ng) using Lipofectamine 3000 (Invitrogen) according to the manufacturer's instructions. After 48 h of incubation, cells were lysed and luciferase activity was measured using a dual luciferase reporter assay system (Promega) and normalized to *Renilla* activity. The pGL3-TK vector (Promega) was used as control. Primers used to generate the 3.0-, 4.2-, and 5.0-kb Runx2 promoter fragments are listed in Table S1.

Author contributions—J. Y. and C.-L. C. conceptualization; J. Y. and C.-L. C. data curation; J. Y., C. W., N. S., X. C., W. Z., and C.-L. C. formal analysis; J. Y. and C.-L. C. supervision; J. Y. and C.-L. C. funding acquisition; J. Y., J. L., J. H., L. Z., C. W., N. S., X. C., W. Z., and C.-L. C. investigation; J. Y. writing-original draft; J. Y. and C.-L. C. writing-review and editing.

Acknowledgments—We thank Dr. Chuxia Deng (National Institutes of Health, NIDDK) for providing Smad4$^{f/f}$ mice and Dr. John Cobb for providing RNA in situ probes (University of Calgary, Canada).

References

1. Rousseau, F., Bonaventure, J., Legeai-Mallet, L., Pelet, A., Rozet, J. M., Maroteaux, P., Le Merrer, M., and Munnich, A. (1994) Mutations in the gene encoding fibroblast growth factor receptor-3 in achondroplasia. *Nature* **371,** 252–254 CrossRef Medline
2. Warman, M. L., Abbott, M., Apte, S. S., Hefferon, T., McIntosh, I., Cohn, D. H., Hecht, J. T., Olsen, B. R., and Francomano, C. A. (1993) A type X collagen mutation causes Schmid metaphyseal chondrodysplasia. *Nat. Genet.* **5,** 79–82 CrossRef Medline
3. Mundlos, S., Otto, F., Mundlos, C., Mulliken, J. B., Aylsworth, A. S., Albright, S., Lindhout, D., Cole, W. G., Henn, W., Knoll, J. H., Owen, M. J., Mertelsmann, R., Zabel, B. U., and Olsen, B. R. (1997) Mutations involving the transcription factor CBFA1 cause cleidocranial dysplasia. *Cell* **89,** 773–779 CrossRef Medline
4. Thomas, J. T., Lin, K., Nandedkar, M., Camargo, M., Cervenka, J., and Luyten, F. P. (1996) A human chondrodysplasia due to a mutation in a TGF-β superfamily member. *Nat. Genet.* **12,** 315–317 CrossRef Medline
5. Karsenty, G., and Wagner, E. F. (2002) Reaching a genetic and molecular understanding of skeletal development. *Dev. Cell* **2,** 389–406 CrossRef Medline
6. Provot, S., and Schipani, E. (2005) Molecular mechanisms of endochondral bone development. *Biochem. Biophys. Res. Commun.* **328,** 658–665 CrossRef Medline
7. de Crombrugghe, B., Lefebvre, V., and Nakashima, K. (2001) Regulatory mechanisms in the pathways of cartilage and bone formation. *Curr. Opin. Cell Biol.* **13,** 721–727 CrossRef Medline
8. de Crombrugghe, B., Lefebvre, V., Behringer, R. R., Bi, W., Murakami, S., and Huang, W. (2000) Transcriptional mechanisms of chondrocyte differentiation. *Matrix Biol.* **19,** 389–394 CrossRef Medline
9. Mackie, E. J., Tatarczuch, L., and Mirams, M. (2011) The skeleton: a multifunctional complex organ: the growth plate chondrocyte and endochondral ossification. *J. Endocrinol* **211,** 109–121 CrossRef Medline
10. Mak, K. K., Kronenberg, H. M., Chuang, P. T., Mackem, S., and Yang, Y. (2008) Indian hedgehog signals independently of PTHrP to promote chondrocyte hypertrophy. *Development* **135,** 1947–1956 CrossRef Medline
11. St-Jacques, B., Hammerschmidt, M., and McMahon, A. P. (1999) Indian hedgehog signaling regulates proliferation and differentiation of chondrocytes and is essential for bone formation. *Genes Dev.* **13,** 2072–2086 CrossRef Medline
12. Yoon, B. S., Pogue, R., Ovchinnikov, D. A., Yoshii, I., Mishina, Y., Behringer, R. R., and Lyons, K. M. (2006) BMPs regulate multiple aspects of growth-plate chondrogenesis through opposing actions on FGF pathways. *Development* **133,** 4667–4678 CrossRef Medline
13. Yoon, B. S., Ovchinnikov, D. A., Yoshii, I., Mishina, Y., Behringer, R. R., and Lyons, K. M. (2005) Bmpr1a and Bmpr1b have overlapping functions and are essential for chondrogenesis *in vivo*. *Proc. Natl. Acad. Sci. U.S.A.* **102,** 5062–5067 CrossRef Medline
14. Shu, B., Zhang, M., Xie, R., Wang, M., Jin, H., Hou, W., Tang, D., Harris, S. E., Mishina, Y., O'Keefe, R. J., Hilton, M. J., Wang, Y., and Chen, D. (2011) BMP2, but not BMP4, is crucial for chondrocyte proliferation and maturation during endochondral bone development. *J. Cell Sci.* **124,** 3428–3440 CrossRef Medline
15. Yoshida, C. A., Yamamoto, H., Fujita, T., Furuichi, T., Ito, K., Inoue, K., Yamana, K., Zanma, A., Takada, K., Ito, Y., and Komori, T. (2004) Runx2 and Runx3 are essential for chondrocyte maturation, and Runx2 regulates limb growth through induction of Indian hedgehog. *Genes Dev.* **18,** 952–963 CrossRef Medline
16. Kim, I. S., Otto, F., Zabel, B., and Mundlos, S. (1999) Regulation of chondrocyte differentiation by Cbfa1. *Mech. Dev.* **80,** 159–170 CrossRef Medline
17. Derynck, R., and Zhang, Y. E. (2003) Smad-dependent and Smad-independent pathways in TGF-β family signalling. *Nature* **425,** 577–584 CrossRef Medline
18. Tan, X., Weng, T., Zhang, J., Wang, J., Li, W., Wan, H., Lan, Y., Cheng, X., Hou, N., Liu, H., Ding, J., Lin, F., Yang, R., Gao, X., Chen, D., and Yang, X. (2007) Smad4 is required for maintaining normal murine postnatal bone homeostasis. *J. Cell Sci.* **120,** 2162–2170 CrossRef Medline
19. Zhang, J., Tan, X., Li, W., Wang, Y., Wang, J., Cheng, X., and Yang, X. (2005) Smad4 is required for the normal organization of the cartilage growth plate. *Dev. Biol.* **284,** 311–322 CrossRef Medline
20. Bénazet, J. D., Pignatti, E., Nugent, A., Unal, E., Laurent, F., and Zeller, R. (2012) Smad4 is required to induce digit ray primordia and to initiate the aggregation and differentiation of chondrogenic progenitors in mouse limb buds. *Development* **139,** 4250–4260 CrossRef Medline
21. Salazar, V. S., Zarkadis, N., Huang, L., Norris, J., Grimston, S. K., Mbalaviele, G., and Civitelli, R. (2013) Embryonic ablation of osteoblast Smad4 interrupts matrix synthesis in response to canonical Wnt signaling and causes an osteogenesis-imperfecta-like phenotype. *J. Cell Sci.* **126,** 4974–4984 CrossRef Medline
22. Lee, K. S., Kim, H. J., Li, Q. L., Chi, X. Z., Ueta, C., Komori, T., Wozney, J. M., Kim, E. G., Choi, J. Y., Ryoo, H. M., and Bae, S. C. (2000) Runx2 is a common target of transforming growth factor β1 and bone morphogenetic protein 2, and cooperation between Runx2 and Smad5 induces osteoblast-specific gene expression in the pluripotent mesenchymal precursor cell line C2C12. *Mol. Cell. Biol.* **20,** 8783–8792 CrossRef Medline
23. Zhang, Y. W., Yasui, N., Ito, K., Huang, G., Fujii, M., Hanai, J., Nogami, H., Ochi, T., Miyazono, K., and Ito, Y. (2000) A RUNX2/PEBP2α A/CBFA1 mutation displaying impaired transactivation and Smad interaction in cleidocranial dysplasia. *Proc. Natl. Acad. Sci. U.S.A.* **97,** 10549–10554 CrossRef Medline
24. Yan, J., Zhang, L., Xu, J., Sultana, N., Hu, J., Cai, X., Li, J., Xu, P. X., and Cai, C. L. (2014) Smad4 regulates ureteral smooth muscle cell differentiation during mouse embryogenesis. *PLoS ONE* **9,** e104503 CrossRef Medline
25. Soriano, P. (1999) Generalized lacZ expression with the ROSA26 Cre reporter strain. *Nat. Genet.* **21,** 70–71 CrossRef Medline
26. Madisen, L., Zwingman, T. A., Sunkin, S. M., Oh, S. W., Zariwala, H. A., Gu, H., Ng, L. L., Palmiter, R. D., Hawrylycz, M. J., Jones, A. R., Lein, E. S., and Zeng, H. (2010) A robust and high-throughput Cre reporting and characterization system for the whole mouse brain. *Nat. Neurosci.* **13,** 133–140 CrossRef Medline

27. Yang, X., Li, C., Herrera, P. L., and Deng, C. X. (2002) Generation of Smad4/Dpc4 conditional knockout mice. *Genesis* **32,** 80–81 CrossRef Medline
28. Shukunami, C., Iyama, K., Inoue, H., and Hiraki, Y. (1999) Spatiotemporal pattern of the mouse chondromodulin-I gene expression and its regulatory role in vascular invasion into cartilage during endochondral bone formation. *Int. J. Dev. Biol.* **43,** 39–49 Medline
29. Jeon, J., Oh, H., Lee, G., Ryu, J. H., Rhee, J., Kim, J. H., Chung, K. H., Song, W. K., Chun, C. H., and Chun, J. S. (2011) Cytokine-like 1 knock-out mice (Cytl1−/−) show normal cartilage and bone development but exhibit augmented osteoarthritic cartilage destruction. *J. Biol. Chem.* **286,** 27206–27213 CrossRef Medline
30. Zheng, Q., Zhou, G., Morello, R., Chen, Y., Garcia-Rojas, X., and Lee, B. (2003) Type X collagen gene regulation by Runx2 contributes directly to its hypertrophic chondrocyte-specific expression *in vivo*. *J. Cell Biol.* **162,** 833–842 CrossRef Medline
31. Li, F., Lu, Y., Ding, M., Napierala, D., Abbassi, S., Chen, Y., Duan, X., Wang, S., Lee, B., and Zheng, Q. (2011) Runx2 contributes to murine *Col10a1* gene regulation through direct interaction with its cis-enhancer. *J. Bone Miner. Res.* **26,** 2899–2910 CrossRef Medline
32. Bond, S. R., Lau, A., Penuela, S., Sampaio, A. V., Underhill, T. M., Laird, D. W., and Naus, C. C. (2011) Pannexin 3 is a novel target for Runx2, expressed by osteoblasts and mature growth plate chondrocytes. *J. Bone Miner. Res.* **26,** 2911–2922 CrossRef Medline
33. Iwamoto, T., Nakamura, T., Doyle, A., Ishikawa, M., de Vega, S., Fukumoto, S., and Yamada, Y. (2010) Pannexin 3 regulates intracellular ATP/cAMP levels and promotes chondrocyte differentiation. *J. Biol. Chem.* **285,** 18948–18958 CrossRef Medline
34. Li, H., and Durbin, R. (2009) Fast and accurate short read alignment with Burrows-Wheeler transform. *Bioinformatics* **25,** 1754–1760 CrossRef Medline
35. Wang, L., Feng, Z., Wang, X., Wang, X., and Zhang, X. (2010) DEGseq: an R package for identifying differentially expressed genes from RNA-seq data. *Bioinformatics* **26,** 136–138 CrossRef Medline
36. Huang da, W., Sherman, B. T., and Lempicki, R. A. (2009) Systematic and integrative analysis of large gene lists using DAVID bioinformatics resources. *Nat. Protoc.* **4,** 44–57 CrossRef Medline
37. Domowicz, M. S., Cortes, M., Henry, J. G., and Schwartz, N. B. (2009) Aggrecan modulation of growth plate morphogenesis. *Dev. Biol.* **329,** 242–257 CrossRef Medline
38. Lefebvre, V., Huang, W., Harley, V. R., Goodfellow, P. N., and de Crombrugghe, B. (1997) SOX9 is a potent activator of the chondrocyte-specific enhancer of the proα1(II) collagen gene. *Mol. Cell. Biol.* **17,** 2336–2346 CrossRef Medline
39. Iwata, T., Chen, L., Li, C., Ovchinnikov, D. A., Behringer, R. R., Francomano, C. A., and Deng, C. X. (2000) A neonatal lethal mutation in FGFR3 uncouples proliferation and differentiation of growth plate chondrocytes in embryos. *Hum. Mol. Genet.* **9,** 1603–1613 CrossRef Medline
40. Nishimura, R., Wakabayashi, M., Hata, K., Matsubara, T., Honma, S., Wakisaka, S., Kiyonari, H., Shioi, G., Yamaguchi, A., Tsumaki, N., Akiyama, H., and Yoneda, T. (2012) Osterix regulates calcification and degradation of chondrogenic matrices through matrix metalloproteinase 13 (MMP13) expression in association with transcription factor Runx2 during endochondral ossification. *J. Biol. Chem.* **287,** 33179–33190 CrossRef Medline
41. Feng, J., Liu, T., Qin, B., Zhang, Y., and Liu, X. S. (2012) Identifying ChIP-seq enrichment using MACS. *Nat. Protoc.* **7,** 1728–1740 CrossRef Medline
42. Qin, H., Chan, M. W., Liyanarachchi, S., Balch, C., Potter, D., Souriraj, I. J., Cheng, A. S., Agosto-Perez, F. J., Nikonova, E. V., Yan, P. S., Lin, H. J., Nephew, K. P., Saltz, J. H., Showe, L. C., Huang, T. H., and Davuluri, R. V. (2009) An integrative ChIP-chip and gene expression profiling to model SMAD regulatory modules. *BMC Syst. Biol.* **3,** 73 CrossRef Medline
43. Jonk, L. J., Itoh, S., Heldin, C. H., ten Dijke, P., and Kruijer, W. (1998) Identification and functional characterization of a Smad binding element (SBE) in the JunB promoter that acts as a transforming growth factor-β, activin, and bone morphogenetic protein-inducible enhancer. *J. Biol. Chem.* **273,** 21145–21152 CrossRef Medline
44. Heinz, S., Benner, C., Spann, N., Bertolino, E., Lin, Y. C., Laslo, P., Cheng, J. X., Murre, C., Singh, H., and Glass, C. K. (2010) Simple combinations of lineage-determining transcription factors prime cis-regulatory elements required for macrophage and B cell identities. *Mol. Cell* **38,** 576–589 CrossRef Medline
45. Robinson, J. T., Thorvaldsdóttir, H., Winckler, W., Guttman, M., Lander, E. S., Getz, G., and Mesirov, J. P. (2011) Integrative genomics viewer. *Nat. Biotechnol* **29,** 24–26 CrossRef Medline
46. Logan, M., Martin, J. F., Nagy, A., Lobe, C., Olson, E. N., and Tabin, C. J. (2002) Expression of Cre recombinase in the developing mouse limb bud driven by a Prxl enhancer. *Genesis* **33,** 77–80 CrossRef Medline
47. Ovchinnikov, D. A., Deng, J. M., Ogunrinu, G., and Behringer, R. R. (2000) Col2a1-directed expression of Cre recombinase in differentiating chondrocytes in transgenic mice. *Genesis* **26,** 145–146 CrossRef Medline
48. Leung, V. Y., Gao, B., Leung, K. K., Melhado, I. G., Wynn, S. L., Au, T. Y., Dung, N. W., Lau, J. Y., Mak, A. C., Chan, D., and Cheah, K. S. (2011) SOX9 governs differentiation stage-specific gene expression in growth plate chondrocytes via direct concomitant transactivation and repression. *PLoS Genet.* **7,** e1002356 CrossRef Medline
49. Akiyama, H., Chaboissier, M. C., Martin, J. F., Schedl, A., and de Crombrugghe, B. (2002) The transcription factor Sox9 has essential roles in successive steps of the chondrocyte differentiation pathway and is required for expression of Sox5 and Sox6. *Genes Dev.* **16,** 2813–2828 CrossRef Medline
50. Bi, W., Deng, J. M., Zhang, Z., Behringer, R. R., and de Crombrugghe, B. (1999) Sox9 is required for cartilage formation. *Nat. Genet.* **22,** 85–89 CrossRef Medline
51. Lefebvre, V., Li, P., and de Crombrugghe, B. (1998) A new long form of Sox5 (L-Sox5), Sox6, and Sox9 are coexpressed in chondrogenesis and cooperatively activate the type II collagen gene. *EMBO J.* **17,** 5718–5733 CrossRef Medline
52. Akiyama, H., Stadler, H. S., Martin, J. F., Ishii, T. M., Beachy, P. A., Nakamura, T., and de Crombrugghe, B. (2007) Misexpression of Sox9 in mouse limb bud mesenchyme induces polydactyly and rescues hypodactyly mice. *Matrix Biol.* **26,** 224–233 CrossRef Medline
53. Bell, D. M., Leung, K. K., Wheatley, S. C., Ng, L. J., Zhou, S., Ling, K. W., Sham, M. H., Koopman, P., Tam, P. P., and Cheah, K. S. (1997) SOX9 directly regulates the type-II collagen gene. *Nat. Genet.* **16,** 174–178 CrossRef Medline
54. Sekiya, I., Tsuji, K., Koopman, P., Watanabe, H., Yamada, Y., Shinomiya, K., Nifuji, A., and Noda, M. (2000) SOX9 enhances aggrecan gene promoter/enhancer activity and is up-regulated by retinoic acid in a cartilage-derived cell line, TC6. *J. Biol. Chem.* **275,** 10738–10744 CrossRef Medline
55. Inada, M., Yasui, T., Nomura, S., Miyake, S., Deguchi, K., Himeno, M., Sato, M., Yamagiwa, H., Kimura, T., Yasui, N., Ochi, T., Endo, N., Kitamura, Y., Kishimoto, T., and Komori, T. (1999) Maturational disturbance of chondrocytes in Cbfa1-deficient mice. *Dev. Dyn.* **214,** 279–290 CrossRef Medline
56. Takeda, S., Bonnamy, J. P., Owen, M. J., Ducy, P., and Karsenty, G. (2001) Continuous expression of Cbfa1 in nonhypertrophic chondrocytes uncovers its ability to induce hypertrophic chondrocyte differentiation and partially rescues Cbfa1-deficient mice. *Genes Dev.* **15,** 467–481 CrossRef Medline
57. Enomoto, H., Enomoto-Iwamoto, M., Iwamoto, M., Nomura, S., Himeno, M., Kitamura, Y., Kishimoto, T., and Komori, T. (2000) Cbfa1 is a positive regulatory factor in chondrocyte maturation. *J. Biol. Chem.* **275,** 8695–8702 CrossRef Medline
58. Komori, T., Yagi, H., Nomura, S., Yamaguchi, A., Sasaki, K., Deguchi, K., Shimizu, Y., Bronson, R. T., Gao, Y. H., Inada, M., Sato, M., Okamoto, R., Kitamura, Y., Yoshiki, S., and Kishimoto, T. (1997) Targeted disruption of Cbfa1 results in a complete lack of bone formation owing to maturational arrest of osteoblasts. *Cell* **89,** 755–764 CrossRef Medline
59. Otto, F., Thornell, A. P., Crompton, T., Denzel, A., Gilmour, K. C., Rosewell, I. R., Stamp, G. W., Beddington, R. S., Mundlos, S., Olsen, B. R., Selby, P. B., and Owen, M. J. (1997) Cbfa1, a candidate gene for cleidocranial dysplasia syndrome, is essential for osteoblast differentiation and bone development. *Cell* **89,** 765–771 CrossRef Medline

60. Nishio, Y., Dong, Y., Paris, M., O'Keefe, R. J., Schwarz, E. M., and Drissi, H. (2006) Runx2-mediated regulation of the zinc finger *Osterix*/*Sp7* gene. *Gene* **372,** 62–70 CrossRef Medline
61. Deng, C., Wynshaw-Boris, A., Zhou, F., Kuo, A., and Leder, P. (1996) Fibroblast growth factor receptor 3 is a negative regulator of bone growth. *Cell* **84,** 911–921 CrossRef Medline
62. Lee, K. S., Hong, S. H., and Bae, S. C. (2002) Both the Smad and p38 MAPK pathways play a crucial role in Runx2 expression following induction by transforming growth factor-β and bone morphogenetic protein. *Oncogene* **21,** 7156–7163 CrossRef Medline
63. Terpstra, L., Prud'homme, J., Arabian, A., Takeda, S., Karsenty, G., Dedhar, S., and St-Arnaud, R. (2003) Reduced chondrocyte proliferation and chondrodysplasia in mice lacking the integrin-linked kinase in chondrocytes. *J. Cell Biol.* **162,** 139–148 CrossRef Medline
64. Long, F., Zhang, X. M., Karp, S., Yang, Y., and McMahon, A. P. (2001) Genetic manipulation of hedgehog signaling in the endochondral skeleton reveals a direct role in the regulation of chondrocyte proliferation. *Development* **128,** 5099–5108 Medline
65. Retting, K. N., Song, B., Yoon, B. S., and Lyons, K. M. (2009) BMP canonical Smad signaling through Smad1 and Smad5 is required for endochondral bone formation. *Development* **136,** 1093–1104 CrossRef Medline
66. Saito, A., Kanemoto, S., Zhang, Y., Asada, R., Hino, K., and Imaizumi, K. (2014) Chondrocyte proliferation regulated by secreted luminal domain of ER stress transducer BBF2H7/CREB3L2. *Mol. Cell* **53,** 127–139 CrossRef Medline
67. Cai, C. L., Martin, J. C., Sun, Y., Cui, L., Wang, L., Ouyang, K., Yang, L., Bu, L., Liang, X., Zhang, X., Stallcup, W. B., Denton, C. P., McCulloch, A., Chen, J., and Evans, S. M. (2008) A myocardial lineage derives from Tbx18 epicardial cells. *Nature* **454,** 104–108 CrossRef Medline
68. McLeod, M. J. (1980) Differential staining of cartilage and bone in whole mouse fetuses by Alcian blue and Alizarin red S. *Teratology* **22,** 299–301 CrossRef Medline
69. Cai, X., Zhang, W., Hu, J., Zhang, L., Sultana, N., Wu, B., Cai, W., Zhou, B., and Cai, C. L. (2013) Tbx20 acts upstream of Wnt signaling to regulate endocardial cushion formation and valve remodeling during mouse cardiogenesis. *Development* **140,** 3176–3187 CrossRef Medline